

# Shadow levels

Benjamin Ménétrier

Last update: October 29, 2024

Copyright ©2024: Meteorologisk Institutt

## Contents

<b>1</b>	<b>Motivation</b>	<b>1</b>
<b>2</b>	<b>Theory</b>	<b>1</b>
2.1	General framework . . . . .	1
2.2	Shadow levels operators . . . . .	2
2.3	Compactly supported functions . . . . .	3
<b>3</b>	<b>Illustration</b>	<b>3</b>
3.1	Local orography . . . . .	3
3.2	Shadow levels weights . . . . .	3
3.3	Dirac test at low altitude . . . . .	4
3.4	Dirac test at high altitude . . . . .	4
3.5	Comparison with a full 3D convolution . . . . .	4

## 1 Motivation

For the convolution of 2D variables in correlation/localization implementations, orography can be very important (e.g. for snow over mountains). However, full 3D convolution is costly for two reasons: coefficients computation and normalization. It would be much more efficient to use existing horizontal convolution implementations (spectral, recursive filters, etc.) with an extra step to take orography into account.

## 2 Theory

### 2.1 General framework

The proposed solution is to surround a 3D horizontal convolution operator with shadow levels extension and reduction operators (mutually adjoint):

$$\mathbf{C}_{2D} = \mathbf{F}\mathbf{C}_{3D}\mathbf{F}^T \quad (1)$$

where:

- $\mathbf{C}_{3D}$  is a 3D horizontal convolution operator,
- $\mathbf{F}$  is the shadow levels reduction operator,
- $\mathbf{F}^T$  is the shadow levels extension operator,
- $\mathbf{C}_{2D}$  is the resulting 2D horizontal convolution operator.

### 2.2 Shadow levels operators

We define the  $K$  shadow levels as vertical levels at constant height  $f_1, \dots, f_K$  in the orography vertical coordinate unit (e.g. meters). For each of the  $n$  horizontal grid-points (listed with index  $i$ ) and each shadow level  $k$ , a weight  $w_k(i)$  is computed as:

$$w_k(i) = \begin{cases} c \left( \frac{f_k - z(i)}{r_v(i)} \right) & \text{if } f_k \geq z(i) \quad [\text{above surface}] \\ 0 & \text{if } f_k < z(i) \quad [\text{below surface}] \end{cases} \quad (2)$$

where:

- $c$  is a convolution function (e.g. Gaspari-Cohn 1999),
- $z(i)$  is the local orography,
- $r_v(i)$  is the local vertical convolution length-scale.

Weights are rescaled to ensure  $\mathbf{C}_{2D}$  normalization:

$$\bar{w}_k(i) = \sqrt{\frac{w_k(i)}{\sum_{k'=1}^K w_{k'}(i)}} \quad (3)$$

and these normalized weights are the diagonal elements of weight matrices  $\mathbf{W}^1, \dots, \mathbf{W}^K$ :

$$\mathbf{W}^k = \begin{pmatrix} \bar{w}_k(1) & 0 & 0 \\ 0 & \ddots & 0 \\ 0 & 0 & \bar{w}_k(n) \end{pmatrix} \quad (4)$$

The reduction operator  $\mathbf{F}$  is given by:

$$\mathbf{F} = \mathbf{RW} \quad (5)$$

where  $\mathbf{R}$  is a reduction matrix, i.e. a row of identity matrices:

$$\mathbf{R} = (\mathbf{I} \ \cdots \ \mathbf{I}) \quad (6)$$

and  $\mathbf{W}$  is the diagonal matrix of weight matrices:

$$\mathbf{W} = \begin{pmatrix} \mathbf{W}^1 & 0 & 0 \\ 0 & \ddots & 0 \\ 0 & 0 & \mathbf{W}^K \end{pmatrix} \quad (7)$$

Consistently, the extension operator is given by:

$$\mathbf{F}^\top = \mathbf{WR}^\top \quad (8)$$

since  $\mathbf{W}$  is diagonal.

If we consider the horizontal field  $T(i)$  and the 3D field  $\hat{T}(i, k)$ :

- the reduction operator  $\mathbf{F}$  reduces  $\hat{T}(i, k)$  into  $T(i)$ :

$$T(i) = \sum_{k=1}^K \bar{w}_k(i) \hat{T}(i, k) \quad (9)$$

- the extension operator  $\mathbf{F}^\top$  extends  $T(i)$  into  $\hat{T}(i, k)$ :

$$\hat{T}(i, k) = \bar{w}_k(i) T(i) \quad (10)$$

## 2.3 Compactly supported functions

For compactly supported functions (like Gaspari-Cohn 1999), and if shadow levels are too far apart, the orography  $z(i)$  can be too far away from the surrounding shadow levels. For example:

- Shadow levels  $f_1$  and  $f_2$  are located at 0 and 100 m, respectively.
- The convolution function  $c$  has a compact support of radius 1.
- The local orography is  $z(i) = 45$  m.
- The local vertical convolution length-scale is  $r_v(i) = 30$  m.

In this case, the weights are:

$$\begin{aligned} f_1 < z(i) &\Rightarrow w_1(i) = 0 \\ f_2 \geq z(i) &\Rightarrow w_2(i) = c \left( \frac{f_2 - z(i)}{r_v(i)} \right) = c \left( \frac{55}{30} \right) = 0 \end{aligned}$$

As a consequence, it is not possible to compute the normalized weights  $\bar{w}$  and to define shadow levels operators. In the practical implementation, an exception should be thrown asking the user either to decrease the vertical distance between shadow levels  $f_1$  and  $f_2$ , or to increase the value of  $r_v(i)$ .

## 3 Illustration

### 3.1 Local orography

With its steep orography, the Sognefjord region (western Norway) is well suited for testing the shadow levels method, as shown in Figure 1

### 3.2 Shadow levels weights

The normalized weights at different altitudes are displayed in Figure 2, showing a clear link to the remaining number of levels above surface:

### 3.3 Dirac test at low altitude

To clearly understand how the shadow levels work, we apply the convolution matrix  $\mathbf{C}_{2D}$  on a Dirac vector  $\delta^j$ :

$$\delta_i^j = \begin{cases} 1 & \text{if } i = j \\ 0 & \text{elsewhere} \end{cases} \quad (11)$$

In the first Dirac test, the impulse is located at a low altitude within the fjord, as shown in Figure 3. Then, the extension operator  $\mathbf{F}^T$  is applied on  $\delta^j$ , as shown in Figure 4. The horizontal 3D convolution operator  $\mathbf{C}_{3D}$  is applied on  $\mathbf{F}^T\delta^j$  to give Figure 5. The weight matrix  $\mathbf{W}$  is applied in Figure 6 and the reduction matrix  $\mathbf{R}$  in Figure 7.

As expected, the resulting increment propagates horizontally following the fjord, but not at higher elevations. In a variational data assimilation system, an observation at the bottom of the fjord would not have any impact on the surrounding hills.

### 3.4 Dirac test at high altitude

The same test can be conducted with a Dirac impulse on a hill, Figures 8, 9, 10, 11 and 12 show the same sequence. In that case, the increment is confined at high altitude. It propagates on surrounding hills, but not to the bottom of the fjord.

### 3.5 Comparison with a full 3D convolution

In Figure 13, we compare the use of shadow levels with the reference of a full 3D convolution (using the BUMP library) at very high horizontal resolution. Both yield very similar results, the shadow levels methods being several orders of magnitude cheaper to run.

# Figures

In all the following figures, the red color map goes from 0 (white) to 1 (dark red).

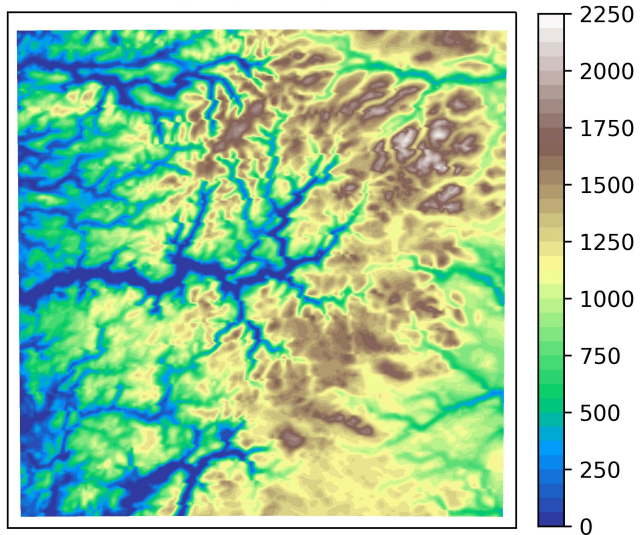


**Figure 1:** Orography of the Sognefjord region (m)

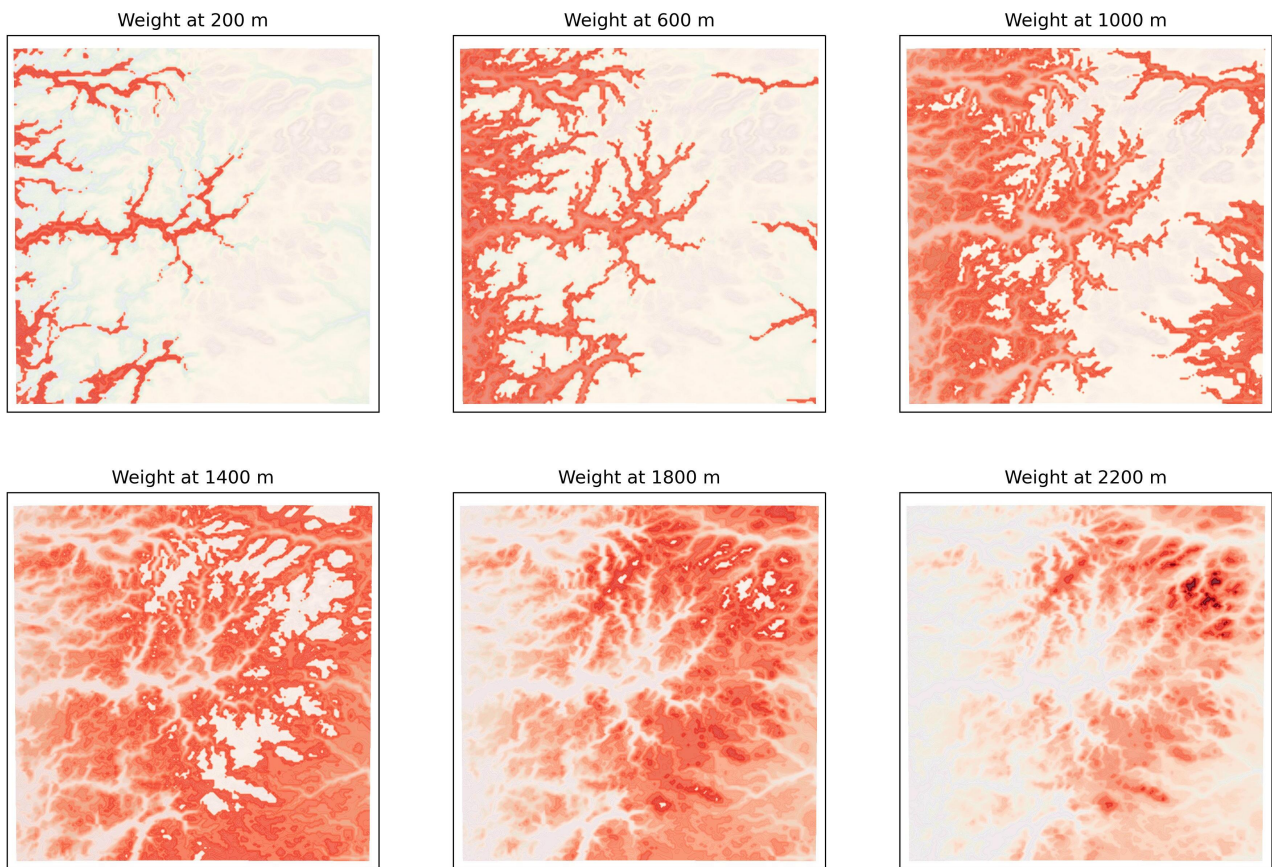


**Figure 2:** Normalized weights  $\bar{w}$  (values ranging from 0 to 1)

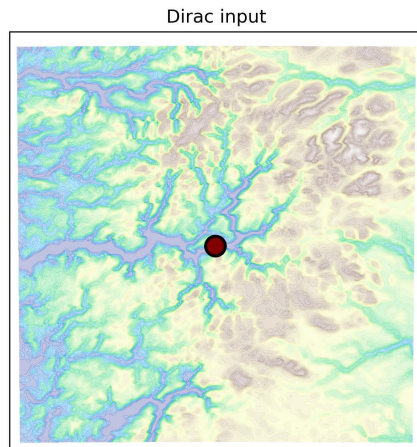


**Figure 3:** Dirac test:  $\delta^j$

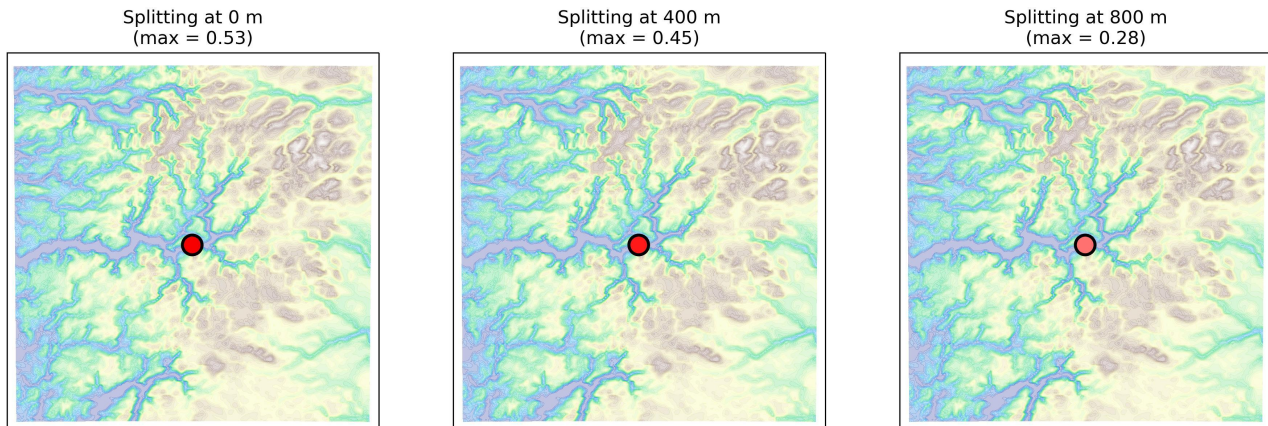


**Figure 4:** Dirac test:  $\mathbf{F}^T \delta^j$

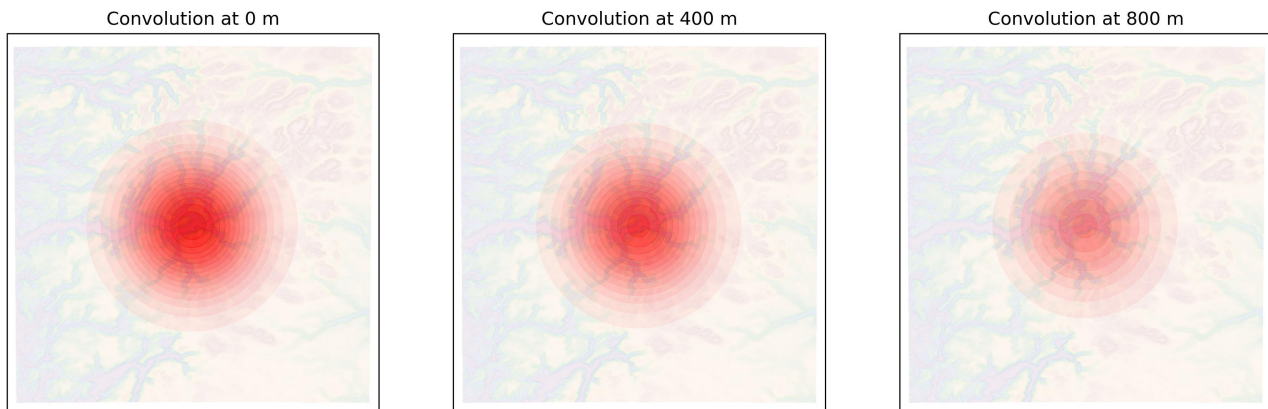


**Figure 5:** Dirac test:  $\mathbf{C}_{3D} \mathbf{F}^T \delta^j$

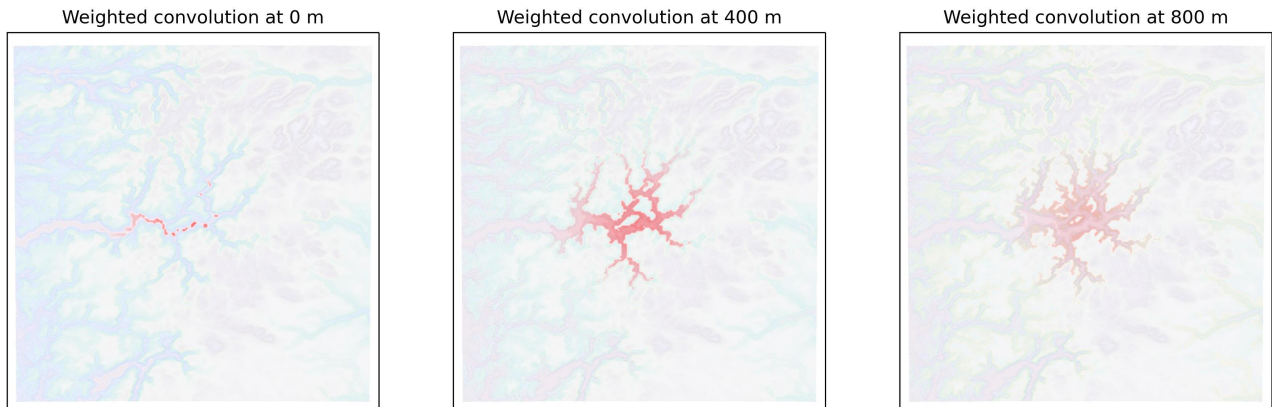


**Figure 6:** Dirac test:  $\mathbf{W}\mathbf{C}_{3D}\mathbf{F}^T\delta^j$

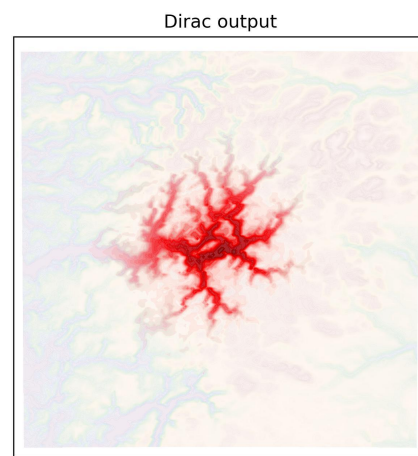


**Figure 7:** Dirac test:  $\mathbf{F}\mathbf{C}_{3D}\mathbf{F}^T\delta^j$

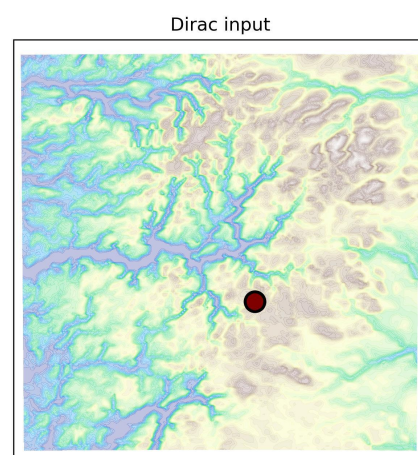


**Figure 8:** Dirac test:  $\delta^j$

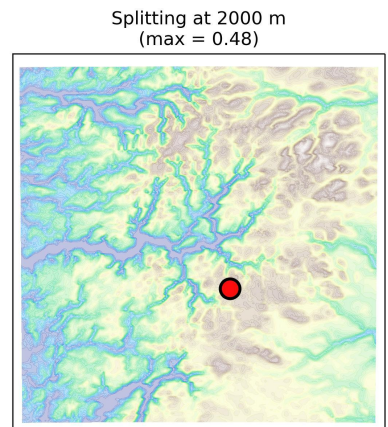
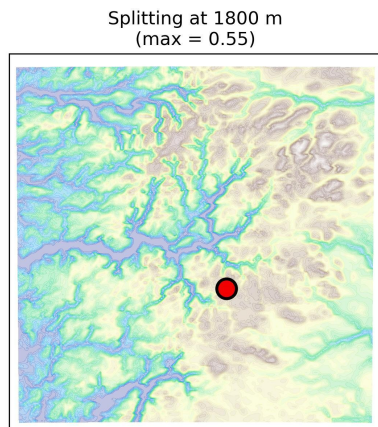
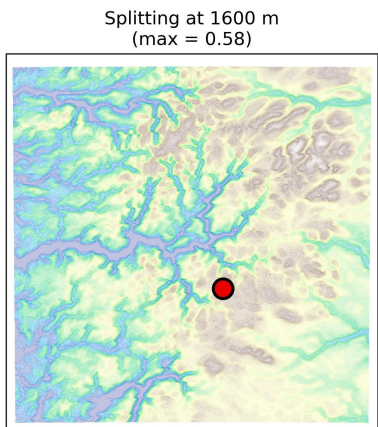


**Figure 9:** Dirac test:  $\mathbf{F}^T \delta^j$

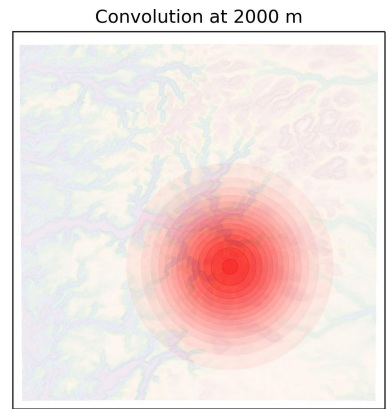
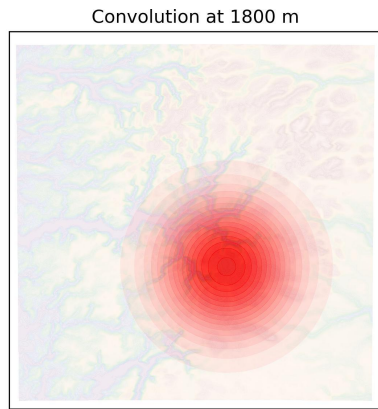
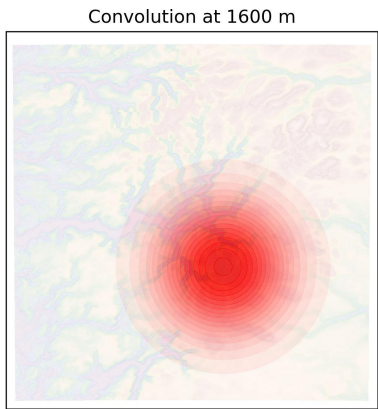


**Figure 10:** Dirac test:  $\mathbf{C}_{3D} \mathbf{F}^T \delta^j$

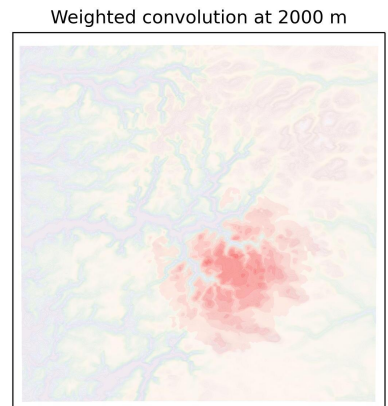
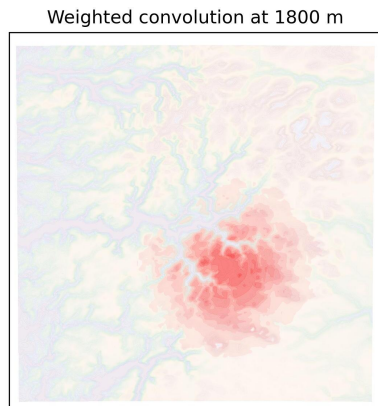
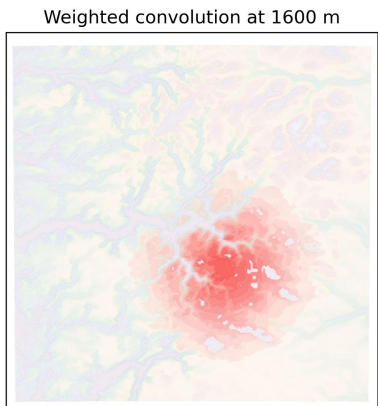


**Figure 11:** Dirac test:  $\mathbf{W}\mathbf{C}_{3D} \mathbf{F}^T \delta^j$

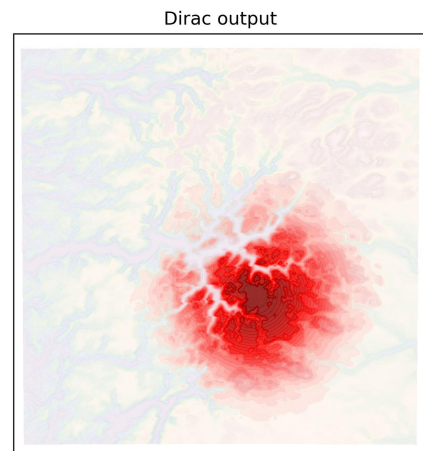


**Figure 12:** Dirac test:  $\mathbf{F}\mathbf{C}_{3D}\mathbf{F}^\top\delta^j$

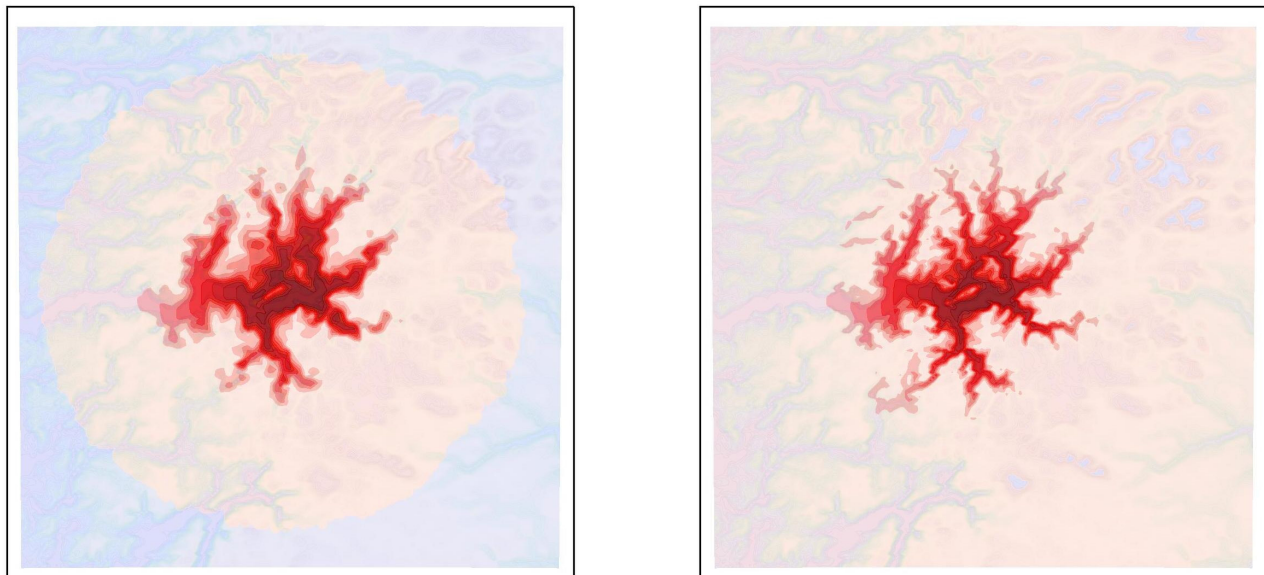


**Figure 13:** Left: full 3D convolution; right: 2D convolution using shadow levels